Lefkada 17/11/2015, Mw 6.4 event: Quick estimate of source complexity

J. Zahradník [1] and E. Sokos [2]

[1] Charles University in Prague, Czech Republic

[2] University of Patras, Greece

Report sent to EMSC on 22/11/2015

The objective of this short report is to summarize the first results indicating source complexity and rupture directivity of the recent Lefkada, western Greece earthquake. The analysis is based on regional seismic data.

Full waveforms are inverted into a point- and multiple-point source models. Moment tensor (MT) is calculated by least-squares fitting of band-pass displacement waveforms, while the source position and time are grid-searched. Multiple sources are computed using iterative deconvolution (Sokos and Zahradník, 2013; Zahradník and Sokos, 2014). We use waveform data from the Hellenic Unified Seismic Network (HUSN) stations at distances 80-200 km. Stations providing a good azimuthal coverage, and being free of instrumental disturbances, were selected. All stations are broad-band, except LTHK, VAR1 and PVO, where strong-motion data were used. Green functions are calculated in a 1D velocity model of Haslinger et al. (1999). The non-automated ISOLA was used for this multi-test investigation; the latest version of the code is available here: http://seismo.geology.upatras.gr/isola/ and http://geo.mff.cuni.cz/~jz/isola_2015/.

We proceed from simple low-frequency source models to more complicated ones. The reference point is the epicenter reported by the Geodynamic Institute of National Observatory of Athens (GINOA) at 38.6655^{o}N , 20.6002^{o}E; the reference time t=0 is chosen at 07:09:47.00 UTC, i.e. 20 s before the origin time reported by NOA (17/11/2015, 07:10:07).

Test 1. Source depth

The source position is initially grid-searched below the reference point at trial depths from 2.2 to 22.2 km (step 1 km) in frequency range 0.01-0.05 Hz; deviatoric MT is assumed. The optimum solution is at dept 5.2 km (with similar correlation values at ~4-7 km), providing variance reduction VR=0.53 and double-couple percentage DC=97%. The solution has a large stability in space and time, with MT varying just slightly around the optimum strike/dip/rake values, here after denoted as s/d/r = 28°/ 79°/-151° (Fig. 1).

Test2. First indication of source complexity

Repeating the same grid search as in Test 1, but using higher frequencies 0.03-0.08 Hz, we obtain similar s/d/r values and similar depth variation of the correlation, but the optimum solution features a very low DC~25%. It indicates that true centroid is horizontally displaced from epicenter and/or the source has some complexity.

Test3. Centroid moment-tensor solution

We perform a horizontal grid search of centroid using frequencies 0.01-0.05 Hz and deviatoric MT inversion. The grid (5 km step) is situated at the depth of 5.2 km and centered at the reference point. The results clearly indicate that the centroid is considerably shifted with respect to the GINOA epicenter: 10 km southward, and 5 km westward (Fig. 2). The optimum solution (Fig. 3) has again the almost same s/d/r values as above, s/d/r = 24°/80°/-149°, DC= 85%, VR= 0.61. Condition number CN=3.6 indicates that the MT resolvability is good. Scalar moment is 0.46e19 Nm, hence moment magnitude is Mw=6.4.

When calculating the moment-rate time function for the present centroid position (single-point model) by non-negative least squares method, it reveals two main contributions: small one 4 seconds after the reference time, and main one, another 4 seconds later. This is analogous to the finding of Zahradnik and Sokos (2014) that if true source process is complex, the time function evaluated at centroid position is a powerful indicator of major subevents. Below in Test 4 we obtain analogous result by an independent method.

Test 4. Multiple point-source model

We investigate possible source complexity on a line, passing through the centroid at azimuth of 20° (20 trial positions, step 3 km), using frequencies 0.03-0.08 Hz. The line is situated at depth of 5.2 km. We did several tests, varying the strike of the line, its depth, frequency range and the results were similar. To stabilize the inversion, now we seek (100%) DC-constrained subevents, but leave their s/d/r angles free. The inversion indicates a possible rupture scenario like the one demonstrated in Fig. 4a.

The process started with an early small moment-release (0.17e19 Nm) in the central part of Lefkada Island, i.e. horizontally close to epicenter. The main moment release episode (0.28e19 Nm) occurred ~ 3-4 seconds later, as far as 15 km in the SSW direction, towards Cephalonia Island.

Finally, a third small moment release (~0.1e19 Nm) occurred at ~4 s after the main one, being situated further to the SSW. Note that the focal mechanisms of the two first subevents (s/d/r = 189°/77°/146° and 27°/79°/-150° for the first and second, respectively) are basically right-lateral strike slips with a small thrust component, similar to the centroid solution; see Fig. 4b. It is to emphasize that leaving free the focal mechanisms in the multiple-source models, their similarity is rather exceptional, and can be understood as an indication that the azimuth of the trial source line is a good approximation of the fault. The two first events were found quite stable as regards their position and focal mechanism when doing additional tests, e.g. adopting deviatoric MT inversion, varying the frequency range (e.g. 0.05-0.10 Hz, or 0.04-0.09 Hz), and varying the depth of the trial source line. The third subevent (the latest one, most displaced to SSW) has been found much less stable.

In order to understand whether the latest subevent actually occurred far SSW, we further stabilize the inversion by assuming constant s/d/r = 20°/ 90°/ -150°, and we are seeking position, time and scalar moment of three subevents (Fig. 5a,b). The test has not only confirmed the previously mentioned stability of the first two events as regards their position and time, but also indicated that, indeed, the third latest subevent did rupture the SSW part of the fault. The parameters of the latter 3-point model are presented in Table 1. The model features VR=0.66 and the obtained waveform fit is shown in Fig.6. Note that the fit is very similar to the one of any model in which just the two first subevents are considered.

	Lon	Lat	Time *	Moment (Nm)
Early small subevent (1^{st})	20.6018	38.7024	4.93	0.157E+19
Later major subevent (2^{nd})	20.5311	38.5500	8.08	0.278E+19
Latest small subevent (3^{rd}) +	20.4841	38.4484	11.83	0.079E+19

* Time is relative to GINOA origin time, + The 3^{rd} subevent is the least stable.

Table 1. Parameters of the 3-point source model derived with *fixed* focal mechanism and depth of 5.2 km.

Conclusion

The tests reported above can be summarized as follows. Two moment release episodes can be very reliably distinguished in the studied Mw 6.4 event. The rupture nucleated near the central part of Lefkada Island with a small moment release near epicenter reported by GINOA. Then, ~3-4 seconds later, a major moment release occurred 10 km southward and 5 km westward from the GINOA epicenter; at a relatively shallow depth ~ 5 km. Both events had a similar focal mechanism, predominantly right-lateral strike slip. Still 3-4 seconds later, and further towards SSW, the rupture process likely ended with the smallest third subevent; its focal mechanism cannot be reliably resolved. This simple source model indicates unilateral rupture propagation.

It appears that a plane passing through the centroid of this report at azimuth ~10°-30° and dip ~ 80° (either west- or east dipping) is a good proxy for creating slip inversion models based on near-source strong motion records (to be reported elsewhere). For example, the fault plane passing through centroid at depth 5.2km, striking at 20° and dipping at 80°, seems suitable, because it almost exactly (with an error as small as 250 m) encompass the GINOA hypocenter at its reported depth of 11km. In other words, such fault plane, hypocenter and centroid would satisfy the H-C condition (Zahradnik et al. 2008).

Results of this analysis also indicate that this earthquake ruptured a part of the Cephalonia - Lefkada strike-slip fault that didn't rupture during the Lefkada 2003 event (for details see Zahradník et al., 2005; Benetatos et al., 2007).

The rupture of the present Lefkada event seems to have stopped its propagation towards Cephalonia at the NNE edge of Paliki peninsula of the Cephalonia Island, almost at the same place were the rupture of the 2014 Cephalonia event(s) stopped its propagation towards Lefkada (Sokos et al., 2015).

Acknowledgment

We acknowledge the waveform data exchange within the Hellenic Unified Seismic Network (HUSN) for the broad band stations used in this work. Figures were created using Generic Mapping Tools. One of the authors (J.Z.) has been supported from the Czech Science Foundation grant GACR-14-04372S.

References

Benetatos Ch., Dreger D. and A. Kiratzi 2007. Complex and segmented rupture of the 14 August 2003 (Mw 6.2) Lefkada (Ionian Islands) earthquake. Bulletin of the Seismological Society of America (BSSA), 97, 1B, 35-51.

Haslinger, F., Kissling, E., Ansorge, J., Hatzfeld, D., Papadimitriou, E., Karakostas, V., Makropoulos, K., Kahle, H.G. and Peter, Y., 1999. 3D crustal structure from local earthquake tomography around the Gulf of Arta (Ionian region, NW Greece). Tectonophysics, 304-3, 201-218, doi:10.1016/S0040-1951(98)00298-4

Sokos, E. and Zahradník, J., 2013. Evaluating centroid moment tensor uncertainty in the new version of ISOLA software. Seismol. Res. Lett., 84-4, 656-665,doi:10.1785/0220130002

Sokos, E., Kiratzi, A., Gallovič, F., Zahradník, J., Serpetsidaki, A., Plicka, V., Janský, J., Kostelecký, J., and G.-A. Tselentis, Rupture process of the 2014 Cephalonia, Greece, earthquake doublet (Mw6) as inferred from regional and local seismic data, Tectonophysics, Volume 656, 12 August 2015, Pages 131-141, ISSN 0040-1951, http://dx.doi.org/10.1016/j.tecto.2015.06.013.

Zahradník, J., Serpetsidaki, A., Sokos E. and Tselentis G-A., 2005: Iterative deconvolution of regional waveforms and a double-event interpretation of the 2003 Lefkada Earthquake, Greece. Bul. Seism. Soc. Am, Vol. 95, No. 1, 159-172.

Zahradnik,J., Gallovic, F., Sokos, E., Serpetsidaki A., and G-A. Tselentis 2008. Quick fault-plane identification by a geometrical method: Application to the Mw 6.2 Leonidio earthquake, 6 January 2008, Greece. Seismological Research Letters Volume 79, Number 5, 653-662

Zahradník, J. and Sokos, E., 2014. The Mw 7.1 Van, Eastern Turkey, earthquake 2011: two-point source modelling by iterative deconvolution and non-negative least squares. Geophys. J. Int., 196-1, 522-538, doi:10.1093/gji/ggt386

Figures

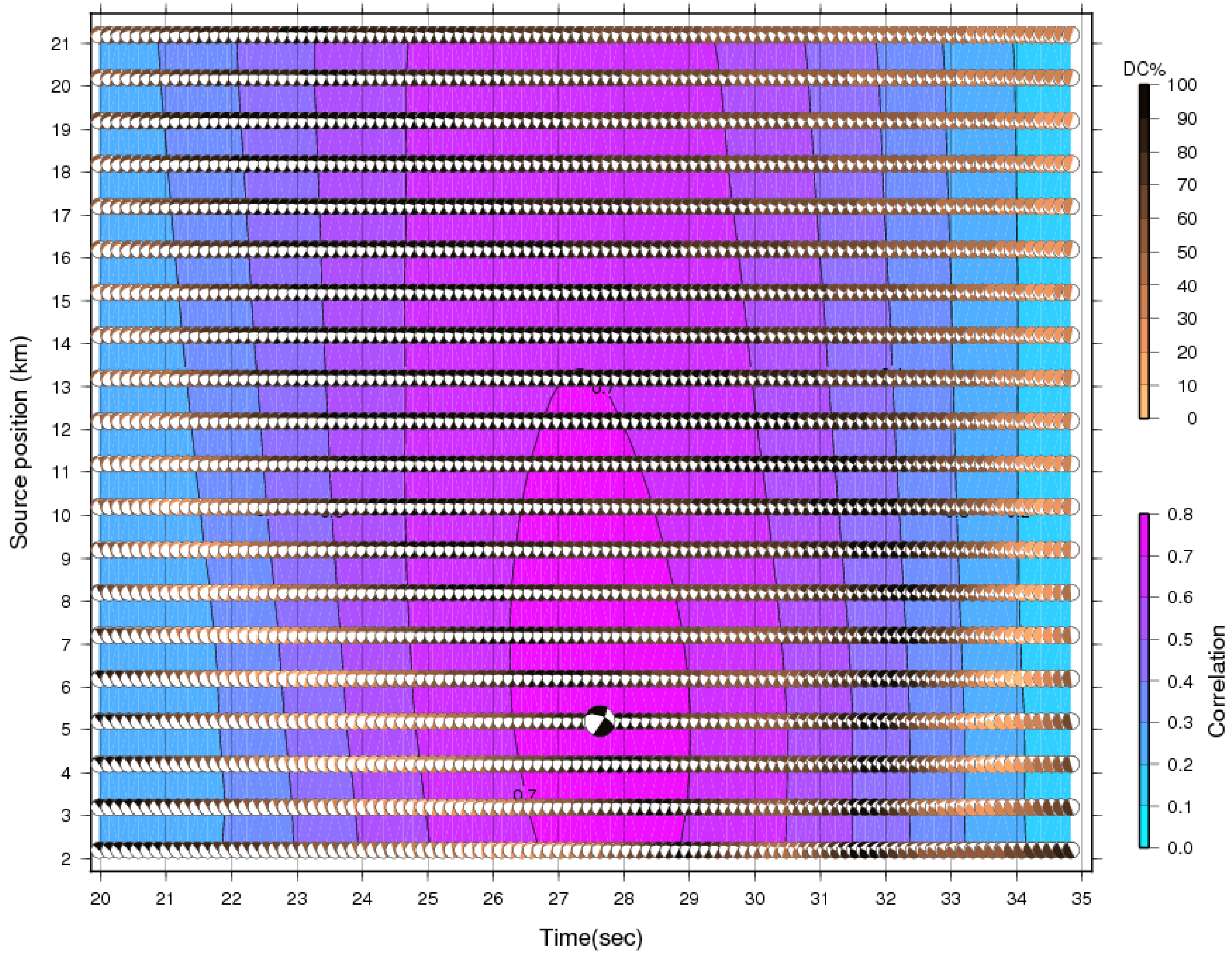

Figure 1. Space-time correlation plot for Test 1. Space position here is the depth below GINOA epicenter. Contours depict correlation between real and synthetic seismograms and color of the beach balls is related to DC%. Time has a formal shift of 20s with respect to GINOA origin time (see text). Optimum solution is shown by the largest beach ball.

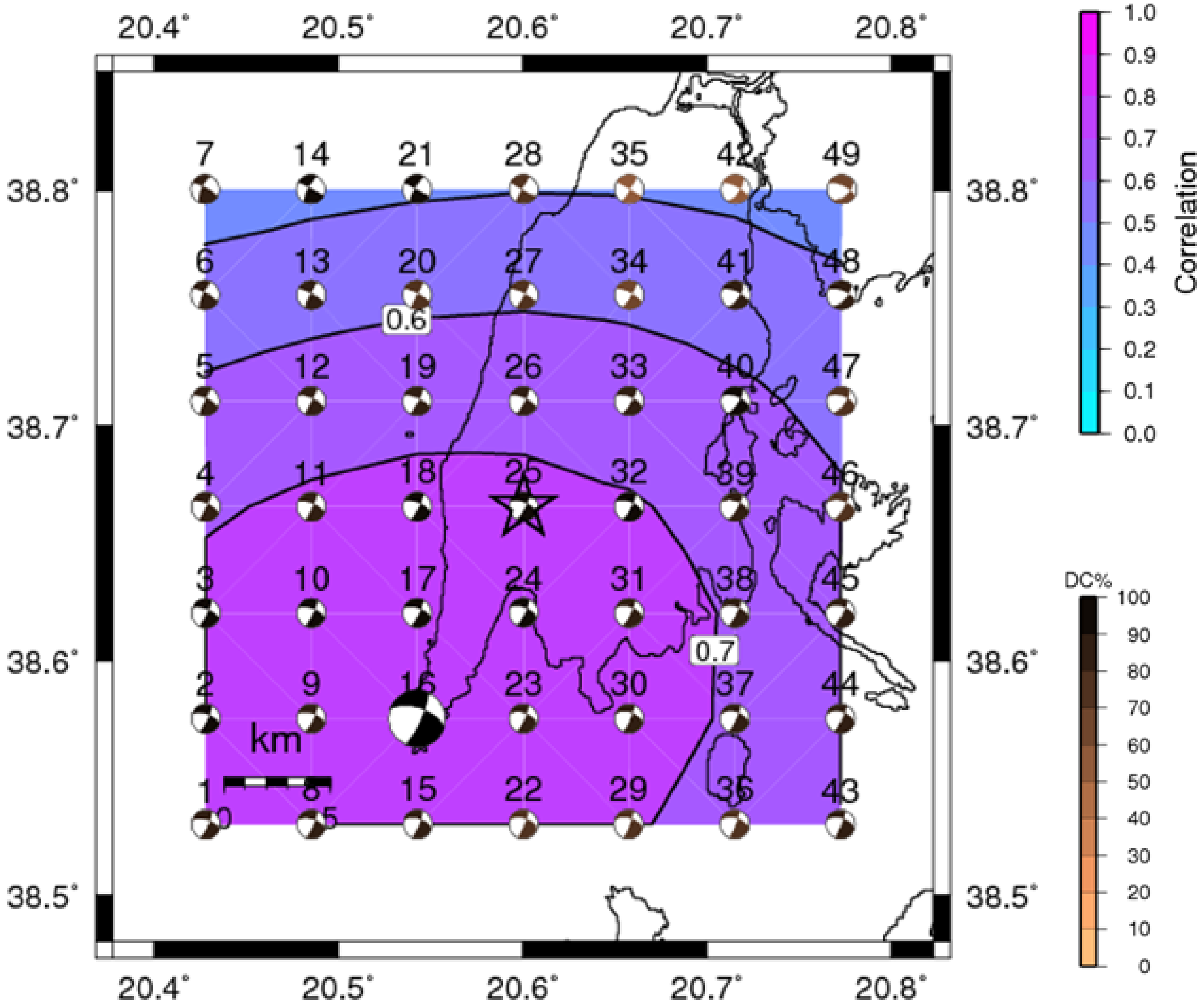

Figure 2. Lat-Lon correlation plot for Test 3, i.e. grid search of centroid and its moment tensor. Point no. 25 in the center is the reference point, i.e. GINOA epicenter. The grid is situated at depth of 5.2 km. (The 0.2 km has been introduced to avoid coincidence with major discontinuity of the velocity model.)

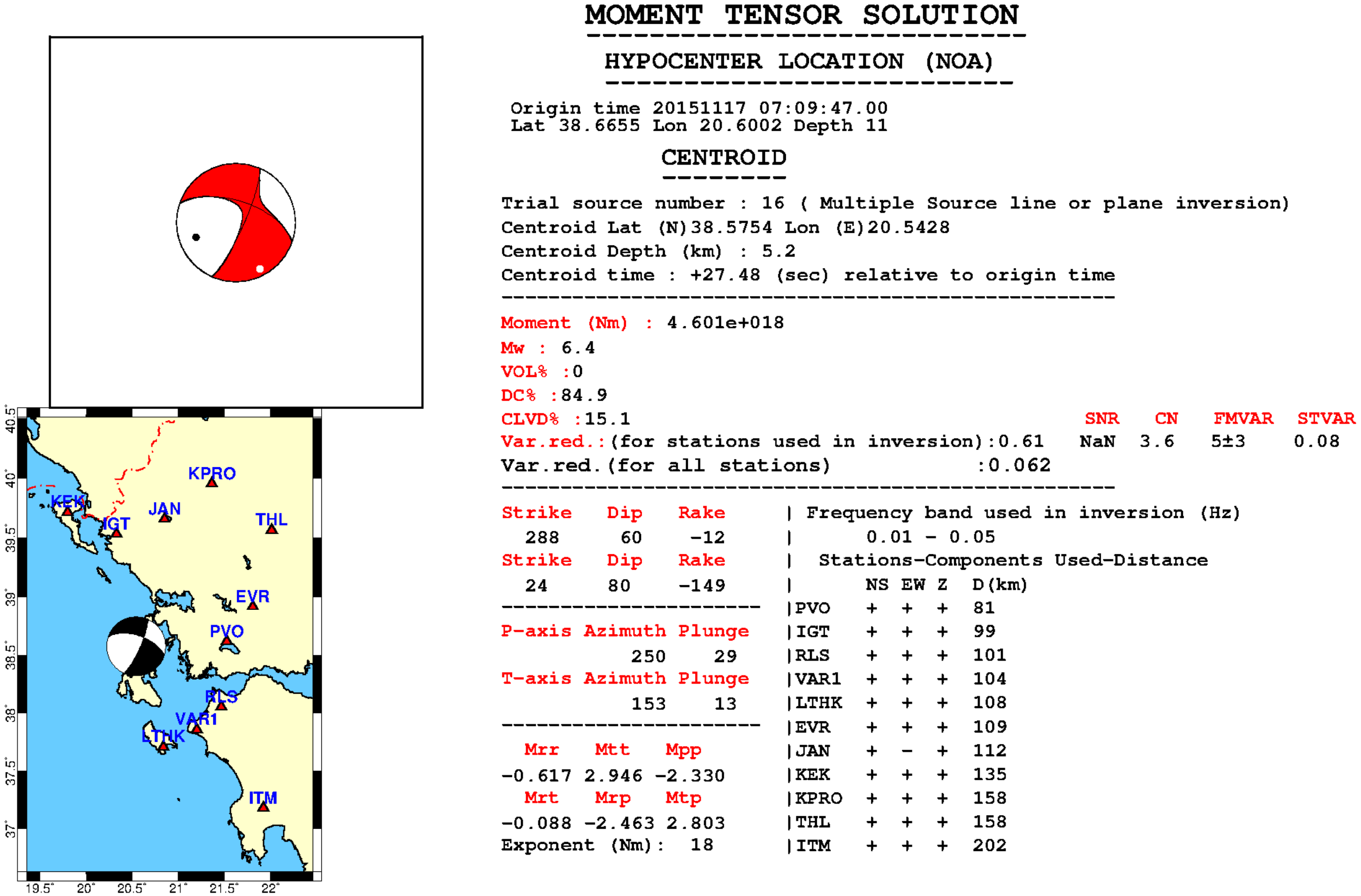

Figure 3. Centroid moment-tensor solution for the Lefkada 17/11/2015 event (Test 3).

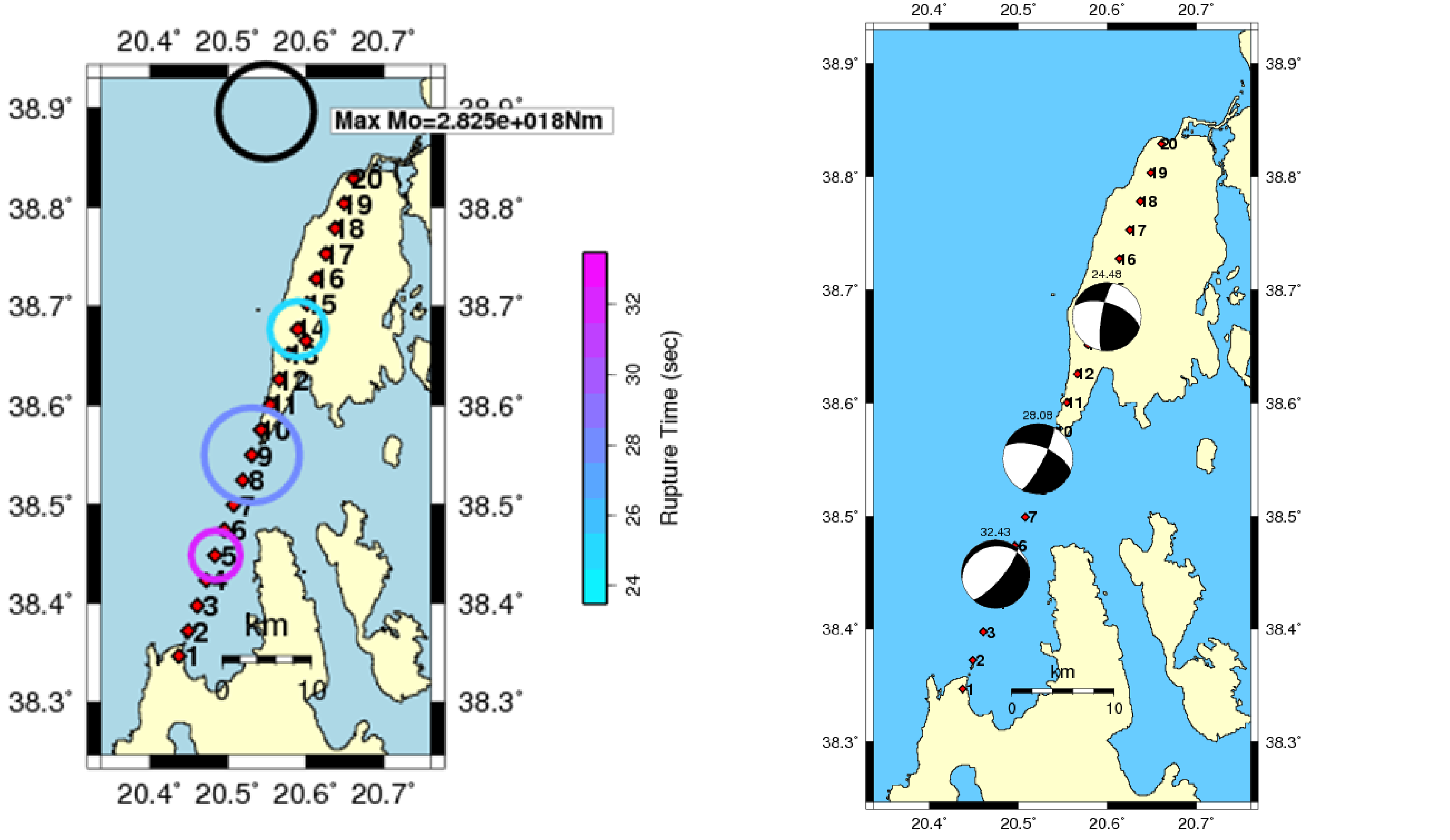

(a) (b)

Figure 4 a) Multiple point-source inversion for the Lefkada event (Test 4 with *DC-constrained* focal mechanisms). Three subevents are shown by circles whose radius scales with moment and color shows rupture time. The time is formally shifted by 20s back with respect to GINOA origin time. b) Focal mechanisms of the subevents, jointly inverted with their position, time and moment; their reliability is limited, mainly as regards the south-west subevent. Numbers above the beach balls indicate their rupture time.

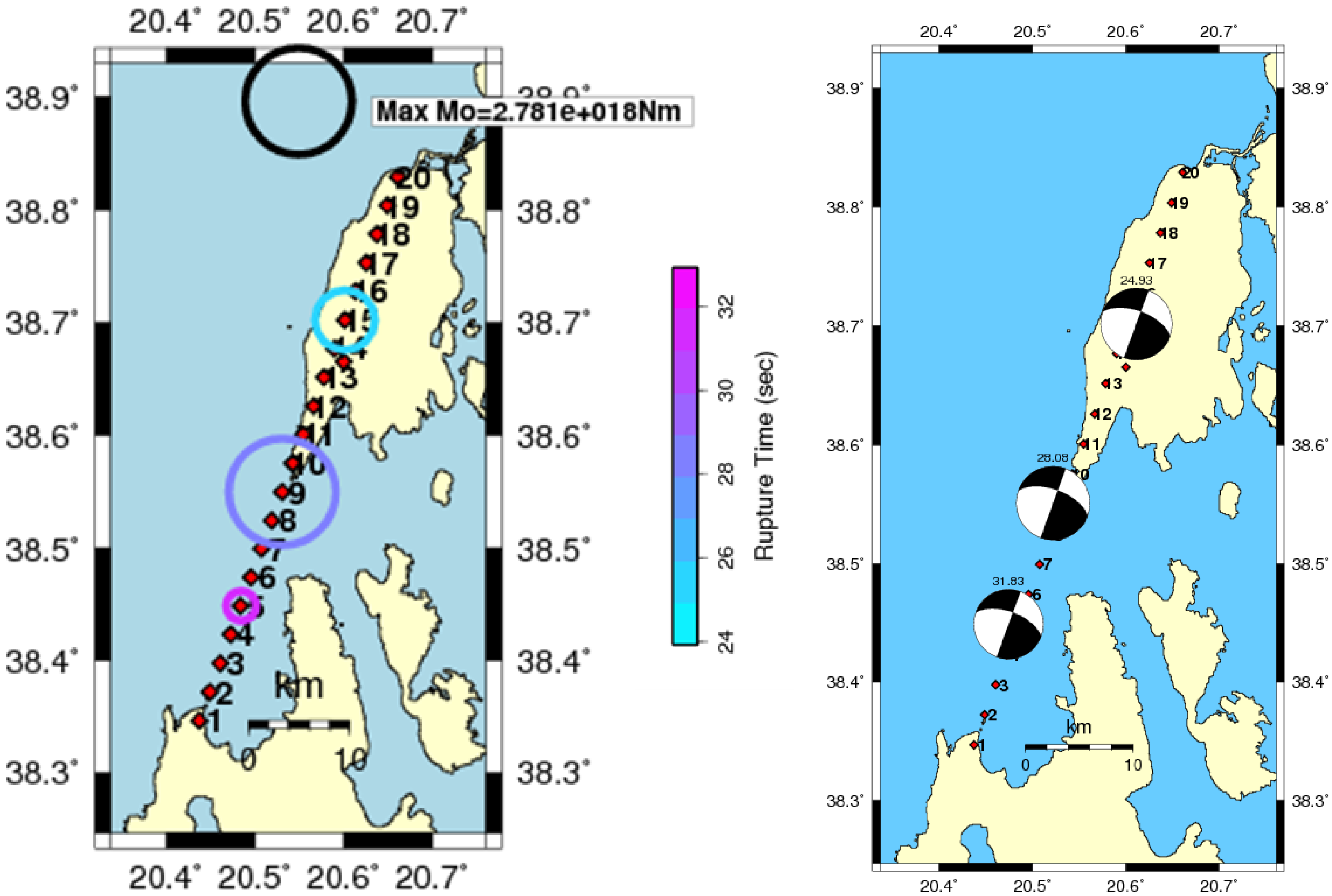

(a) (b)

Figure 5 a) Multiple point-source inversion for the Lefkada event (Test 4 with *constant* focal mechanisms), for legend, see Fig. 4a. b) The assumed constant mechanism is shown by beach balls. For legend details, see Fig. 4b.

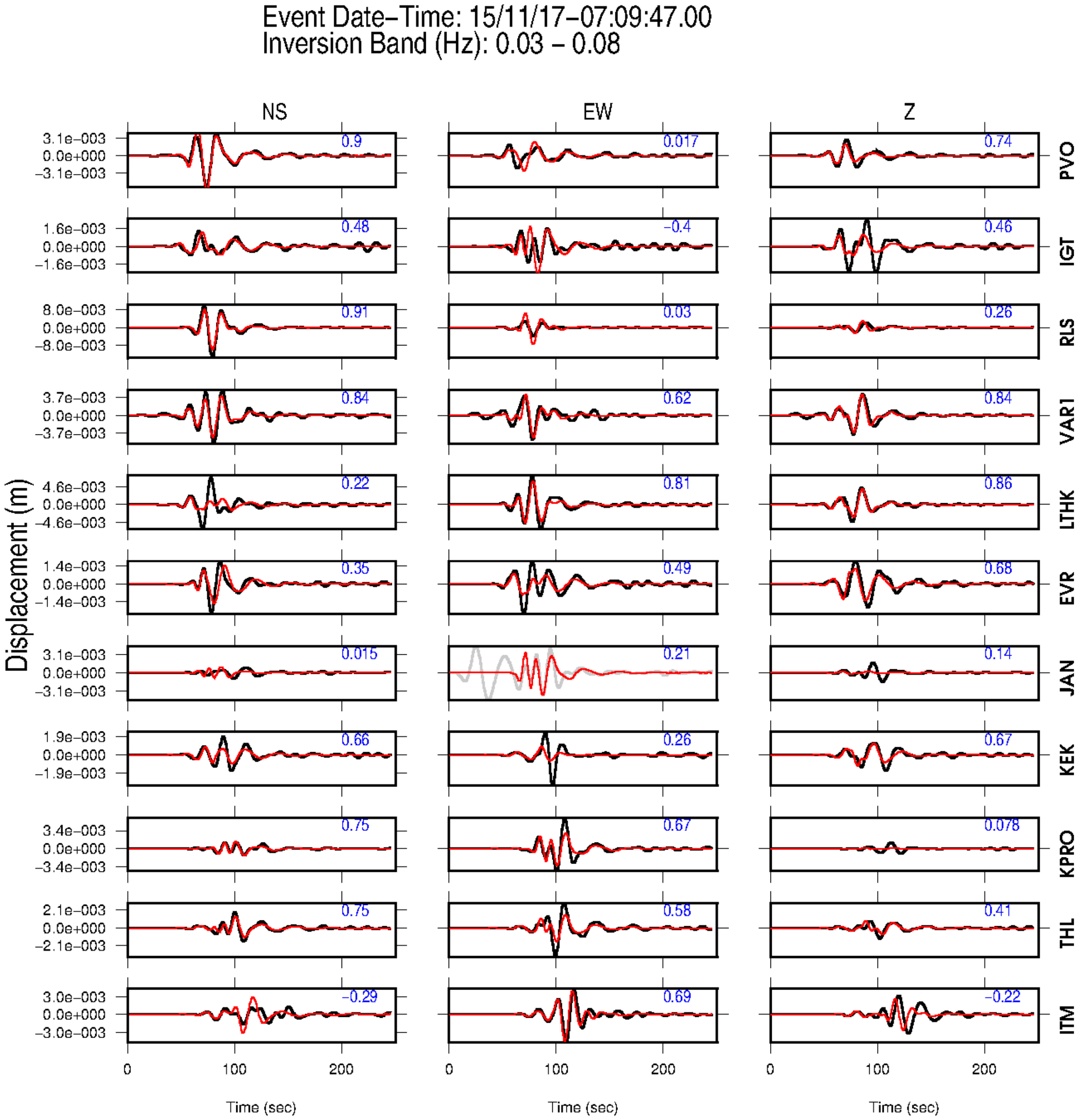

Figure 6. Waveform fit for multiple source inversion of Figs. 5a,b and Table 1. Black and red lines are observed and synthetic displacement data, respectively. The JAN-EW waveform (gray) was not used in the inversion. For the station distribution, see Fig. 3.